Arch. Metall. Mater. **69** (2024), 4, 1543-1554

DOI: https://doi.org/10.24425/amm.2024.151425

B. VINOD[1*], S. SURESH[1], S. SUNIL KUMAR REDDY[1]

TRIBOLOGICAL AND FATIGUE BEHAVIOUR OF Ti-Nb-Zr-Sn ALLOY THROUGH POWDER COMPACTING: NOVEL PERFORMANCE OF HIGH NIOBIUM ALLOYS FOR BONE TISSUE COMPATIBILITY

Biocompatible materials are natural or man-made substances kept in the body to turn a living cell into a working organ. Bone tissue and biocompatibility are emerging as an alternative approach to regenerating bone due to some distinct advantages over autografting and allografting. This research aimed to fabricate a novel porous scaffold Ti-Nb-Zr-Sn alloy that can be utilized as a bone substitute. Ti-Nb-Sn-Zr were selected by different weight ratios and synthesized using the powder metallurgy method. Zirconium (Zr) is incorporated to get enhanced biological performance. The elements Ti, Nb with Zr, and Sn are utilized due to their excellent biocompatibility with the human body. The Ti-35Nb-7Zr-4Sn alloy has high tensile strength between 1042 and 1603 MPa by increasing Zr and Nb weight ratios. In addition, 35% Nb/7% Zr with 4% Sn composite show improved hardness, which is beneficial for resembling bone tissue and die-casting fittings in automobile applications. Fatigue and wear analysis is conducted to help us understand the behaviour of the Ti-Nb-Zr-Sn alloy.

Keywords: Niobium alloy; Biocompatible; Mechanical Properties; Morphological Characterization; Orthopaedic applications

1. Introduction

Bioimplants are intended to assist individuals by replacing or healing damaged tissue. As a result, it is critical to thoroughly understand the materials used for bioimplants and their specific properties and functions. The following criteria are taken into consideration while selecting bio-implant materials [1]. In terms of pharmacological permissibility (non-toxicity and non-carcinogenic), lack of chemical activity and permanence, Benefits including low prices, and simple production. Biocompatible metals like stainless steel, Co-Cr alloys, Ti-Nb alloys, Ni-Ti alloys, and W are utilized for bioimplants. Powders are recommended instead of polymer and ceramics because of their superior formability and biocompatibility. The Ti-Nb-Sn composition has good workability and high corrosive resistance to induce bone tissue. Ronoh et al. [2] stated that, initially, pure titanium was used as an alternative for stainless steel and Co-Cr alloys because of its inherent properties, such as biocompatibility and excellent corrosion resistance. However three major issues were found (a) the modulus of elasticity of Ti (110 GPa) was high as compared to the human bone and (b) high wear loss, and (c) poor mechanical properties as compared to the hard tissues. To overcome these problems, Zr was replaced by α+β Ti-based alloys, especially with Ti-Nb alloy. The mechanical properties of the Ti-Nb-Zr-Sn alloys were in good agreement with the hard tissues still, the cytotoxicity of the alloying elements such as V, and Al caused severe health issues when released into the human body. To overcome the toxicity of V, in this study V free α+β Ti-based alloys such as Ti-Nb-Sn and Ti-Nb-Zr-Sn were developed by replacing V and Al with Zr and Sn. Both these alloys exhibit good mechanical properties when compared to the Ti-6Al-4V. Therefore, low modulus β titanium alloys with β stabilizing elements such as Ta, Nb, Zr, and Sn have been developed because of their non-toxicity [3], enhanced mechanical properties and improved tissue response. Ti-Nb-Sn-Zr alloys show a modulus of elasticity in the range of 48-55 GPa, much lower than the presently used Ti64 conventional alloy [4]. Now-a-days, Zr and Ti form receives much attention for their biological applications; it is used as a biocompatible material for bone implants and is the second-most transplanted tissue in clinics. The zirconium with titanium particulate manufactured by P/M processes, as determined by Alshammari et al. [5], constitutes a kind of low-cost, custom-tailored material with potential uses in the medical field and automotive sectors. Because of the lubricating property,

[1] DEPARTMENT OF MECHANICAL ENGINEERING, SIDDHARTH INSTITUTE OF ENGINEERING & TECHNOLOGY, PUTTUR, INDIA

* Corresponding author: vinod.c2009@gmail.com

titanium in the form of particles is widely used in biocompatible bone regeneration and repair applications.

However, in its biocompatible material form, titanium material is a major organic component of biological hard tissues. Scaffolds for bone have a similar property such as they can sustain typical cellular function, including molecular signalling systems, without causing harm to the host, either locally or systemically [6]. Among other techniques, powder metallurgy plays a vital role because it allows for more precise microstructure control and more feasible reinforcement distribution than casting, as suggested by Balikai et al. [7]. The powder metallurgy combines two powders in the proper ratio before compacting the resulting homogenous mixture, which is a key advantage over casting. The number of people suffering from various degenerative diseases like osteoporosis (bone weakening), osteoarthritis (bone joints inflammation) and trauma has increased tremendously. Preparing implant materials for biomedical applications is a potential solution to these problems [8]. Hence there is a need to restore these functionally compromised structures by substituting them with the artificial implantation of biomaterials of definite shapes. But repeated surgeries are very expensive with a very low success rate. Besides, researchers are still developing material for bone replacement that can help regain the lost structure and function precisely in load-bearing applications. Thus Ti-Nb-Sn-Zr alloy develops implants with a longer lifetime and excellent biocompatibility. The objective of this study is illustrated below:

- Synthesise and develop three biocompatible composites like Ti-35Nb-4Sn alloy, Ti-15Nb-5Zr-4Sn alloy, and Ti-35Nb-7Zr-4Sn alloy potential candidates for biological applications.
- Examine the mechanical alloying using the Powder metallurgy technique.
- To investigate the fatigue and wear behaviour of three Ti-Nb alloys to alleviate the stress shielding effect.
- The mechanical properties and surface morphology of three materials are being studied to find better orthopaedic applications.

2. Experimental details

2.1. Materials

Composites are primarily used in automobile and orthopaedic applications because of their excellent mechanical properties and corrosion resistance. There is an increasing demand for materials with lightweight and load-bearing capabilities for improved performance in hardness and stiffness. A new generation of materials significantly improves temperature capability beyond the operating limits of the conventional superalloys required to meet this demand. Zirconium (Zr) and Titanium (Ti) are abundant elements, ranked as the twentieth most abundant element in the earth's crust. Chen et al. [9] reported that zirconium is a possible replacement or combination with vanadium and aluminium as an alloying element for its strong corrosion resistance in steel. Zr has an inherent affinity with oxygen and nitrogen to form strong nitride and oxides as precipitates, a potential site for more grain nucleation resulting in fine grain structures and improving mechanical properties. Niobium (Nb) and Tin (Sn) are lightweight and have excellent wear resistance compared to other materials such as copper, brass, and steel. In this work, zirconium and titanium are obtained from Viru Chemical Industries in Chennai, whereas the niobium and tin are procured from Avience Chemicals and Pharmaceuticals Pvt. Ltd., Gujarat, India. The zirconium, titanium, niobium, and tin powders are obtained from the company, as shown in Fig. 1. The physical and mechanical properties of powder mixtures obtained from the company are listed in TABLE 1.

Fig. 1. Raw materials of (a) Titanium, (b) Niobium, (c) zirconium and (d) Tin Powders

TABLE 1

Physical and Mechanical Properties of Ti-Nb-Zr-Sn particles

Properties	Titanium	Zirconium	Niobium	Tin
Density (g/Cm^3)	4.42	4.42	4.42	4.42
Size (μm)	32 to 36	28 to 31	12 to 17	11 to 15
Shape	Spherical	Spherical	Spherical	Round
Color	Grey	White	Black	Grey
Strength (MPa)	321	211	287	187
Microhardness (HRC)	315.8	106.7	142.6	89.3
Elastic modulus (GPa)	113	94	102	33
Poisson's ratio	0.32	0.21	0.24	0.11
Thermal conductivity (W-m.k)	23.9	37.2	41.3	62.7

2.2. Methods

2.2.1. Mixing and blending

Using a high-energy ball mill, powders can be mechanically alloyed (MA) to achieve atomic-level alloying, which is

only possible in the solid state. Mechanical alloying is used to obtain a homogeneous distribution of particles. Titanium, zirconium, tin, and niobium powder were thoroughly mixed in a high-energy ball mill. Ball milling was carried out at room temperature (RT ~ 30°C) for 90 min using Fritch-pulverise-6, as shown in Fig. 2(a). A high-energy ball mill for Zr/Nb/Sn biocomposites is used to mill the powder using the wet milling technique. The powder was sealed in a cylindrical WC (tungsten carbide balls) vial with 50 WC balls of three different diameters. The ball-to-powder weight ratio was maintained at 20:1 (ball weight is 400 g, and powder weight is 20 g), and its level was frequently checked. The solvent powders were then deagglomerated in a mortar and sieved after being dried in a furnace for 2 hours at a temperature of 120°C [10].

2.2.2. Compaction and sintering

Preparing Ti-Nb-based composites is a highly challenging task, and limited information exists in the open literature on processing these alloys. The conventional sintering process is a highly energy-intensive way of preparing these composites. Powders were squeezed in a hydraulic pressing machine with a punch and die of 10 mm diameter and 80 mm height at a pressure of 950 MPa. A hydraulic pressing machine and sintering apparatus were used for compaction, as shown in Fig. 2(b-c). No lubricant was included in the powder due to the Zr and Sn particulate's high activity and reactivity to contamination. Zn stearate in acetone was used to lubricate the punch and die walls before powder filling to allow for sample ejection. The high-density green particles were sintered at a choking time of 60 min at a temperature of 1100°C [11], and the sintered specimens are shown in Fig. 2(d).

2.2.3. Hot Extrusion Process

The hot extrusion process is chosen as secondary processing because it can minimize porosity and enhance mechanical performance. After the sintering process, the Ti/Zr/Nb/Sn biocomposites were inserted through a subsequent process (hot extrusion) using a 150-tonne hydraulic press. The die was heated to 850°C in a furnace and filled with alloy and composite billets for this test. After being saturated for 30 min, the billets were extruded at a ratio of 20:1 at a size of 10 mm × 55 mm. In addition to producing structural forms; the extrusion technique achieves a more uniform particle distribution.

2.4. Mechanical characteristics

(a) Tensile test

The samples were machined from a central portion of the test bar for the tensile tests. ASTM E8M-04 standards [12] were used to prepare the tensile test samples at room temperature. Tensile strength, yield strength, and % elongation of the niobium alloys was measured in a universal tension machine of 50-tonne capacity with a constant speed of 1 mm/min (Model: 1038-VS-T). The tension samples used in the testing were 50 mm long and 10 mm in diameter. The purpose of this gauge mark is to calculate the elongation after a fracture. The samples were

Fig. 2. (a) Ball milling apparatus (Fritch-pulverise-6), (b) Hydraulic pressing machine, (c) High temperature tubular furnace, and (d) Sintered samples

held in place by gripping holding devices with fixed rigidity. The strain absorbed in the specimen was calculated using a strain gauge during loading. The axial tension load is gradually applied to the test speed for standard test specimens at 2 mm/min until it fractures using a hydraulic machine.

(b) Microhardness test

A microhardness test was performed on the hybrid composites' NZ cross section in the surface normal to the FSP direction. Samples were tested using a 100 g load for 15 seconds. The device used for this test is a Vickers digital micro-hardness tester performed according to ASTM E9 standards [13].

(c) Impact test

The samples are machined from a central portion of the test bar. The samples for the impact test are prepared as per the ASTM A370 standard [14]. The dimensions of the samples are 10×10×55 mm (at 45°) and 2 mm depth. Impact tests were conducted using a Charpy impact test machine with a range of 0-300 joules at room temperature. The three samples were conducted for each composition, and the average values are reported in the results.

2.6. Tribology test

The pin-on-disc dry sliding technique is a simple and accurate method for wear analysis for niobium composite samples. The wear resistance of the particulate filler blended with the composite is improved. The equipment can evaluate materials' wear and contact qualities in sliding conditions. The pin can act as a sample, with the disc acting as a counter face, as shown in Fig. 3(a). The thickness of the test specimens was 5 mm, and the height was chosen as 15 mm with a 10 mm width as per the ASTM G 99 standard [15]. The specified parameters included a disc speed of 2.3 m/s and a disc diameter of 100 mm. For varying loads from 10 to 50 N, a constant sliding distance (L) of 1200 m was used, and the calculated rotating speed of 3 m/s was maintained. Wear estimation is conveyed to help decide the measurement of the materials worn away after a wear test. The specific wear loss and COF are estimated and detailed during the tribology test.

2.7. Fatigue behaviour

Fatigue behaviour plays a major role in material science through empirical fatigue life assessment methods developed over the years. The test is carried out on notched and un-notched specimens using an MTS 100 KN Servo-hydraulic machine, as shown in Fig. 3(b). Notched specimens may contain stress raisers in the form of holes or notches supposed to be real-life structures with well-defined geometry. On the other hand, un-notched specimens are measured to identify fatigue properties and provide information on notch sensitivity. However, surface conditions strongly influence the fatigue behaviour of both notched and unnotched specimens. High-cycle fatigue (HCF) is investigated as a function of the notch and un-notch factors in the total number of cycles. The specimens' ends were polished sequentially using grade 800 abrasive paper to prepare for the fatigue tests. The samples were cleaned in acetone before the fatigue test. The samples are cut by ASTM E466 standards [16]. The fatigue test uses a specimen that is 10 mm in diameter and 80 mm in length. The test parameters are chosen as a loading frequency of 3 Hz with a minimum load of 0.5 KN and a stress ratio of 0.5, respectively. The stress amplitude (S) is plotted versus the number of cycles (N) to create the S-N curve (N). Using Basquin's equation, it was possible to characterize the shape of the S-N curve for high-cycle fatigue. Ti-Nb alloys are compared along the S-N curve to determine the effect on fatigue life.

$$S^n N = A \quad (1)$$

where, S – stress, N – number of cycles to failure, A – amplitude

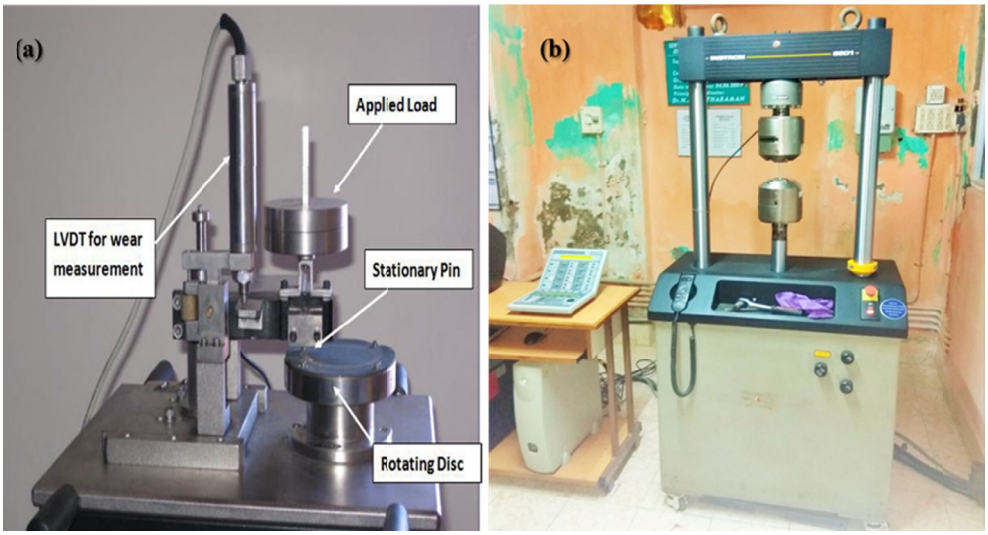

Fig. 3. (a) Pin-on-disc apparatus, and (b) Fatigue test apparatus (MTS 100 KN Servo-hydraulic machine)

2.8. Microstructural examination

Microstructure studies were carried out using scanning electron microscopy and an optical microscope to identify the defects, such as a pin, void, and tunnel in the processed zone. Composite sample failure surface fractography was examined using SEM. The fractured tensile, flexural, and impact biohybrid composite samples are cut and micrographed by the CX-200TM at standard specifications. An ethanol solution is used for each specimen before the SEM analysis. The nature of the material is determined, and fractography is identified at high magnification.

3. Results and discussion

3.1. Optical microscope analysis

The optical microscope images of the Ti-Nb alloys are shown in Fig. 4(a-c). It is observed that the grain size decreased in the order of Ti-35Nb-4Sn > Ti-15Nb-5Zr-4Sn > Ti-35Nb-7Zr-4Sn alloy, and the average grain size is found to be 32.1±23.4, 19.7±6.3, 11.5±3.8, 8.3±2.7 μm respectively. The grains of all samples were further refined after extrusion. This can be attributed to dynamic recrystallization during plastic deformation at high loads. Cracks appear on the surface due to their brittle nature, as shown in Fig. 4a. In general. According to Li et al. [17], hard reinforcement particles increase the durability and influence the grain size of Nb material. Fig. 4(b) optical micrographs of zirconium particles demonstrating dendritic structure. The particle size and weight fraction influence the composite's structure to a greater extent. Increasing the weight percent of Zr and Nb particles tends to minimize the grain size. The reinforcement particles are strongly bonded with the matrix, leading to a homogenous distribution of reinforcement particles on each other at certain places (Fig. 4(c)), and are bonded properly. Adding aligned tin, zirconium, and niobium particles with Ti can minimize the cracks and fracture surface. However, Ti-35Nb-4Sn alloy leads to pores and pits appearing on the material surface, leading to larger grains. The incorporation of 7% Zr particles has a significant effect on material strength. The Ti-35Nb-7Zr-4Sn exhibits small grains and a finer structure than the other alloys.

3.2. Mechanical properties

3.2.1. Hardness test

The results of microhardness test samples of all three alloys are shown in Fig. 5. The Ti-Nb surface layer appeared as particles well dispersed in the layer of the composite mixing zone and well bound to the alloy surface without any defect formation. The Ti-35Nb-4Sn possesses a minimum microhardness value of 438.71 HV, and Ti-15Nb-5Zr-4Sn is 456.53 HV. Among other samples, the Ti-35Nb-7Zr-4Sn exhibits a higher hardness of 479.83 HV. The increased amount of 4% Sn with 35% Nb particles to Ti strengthened the base material, and the 7%

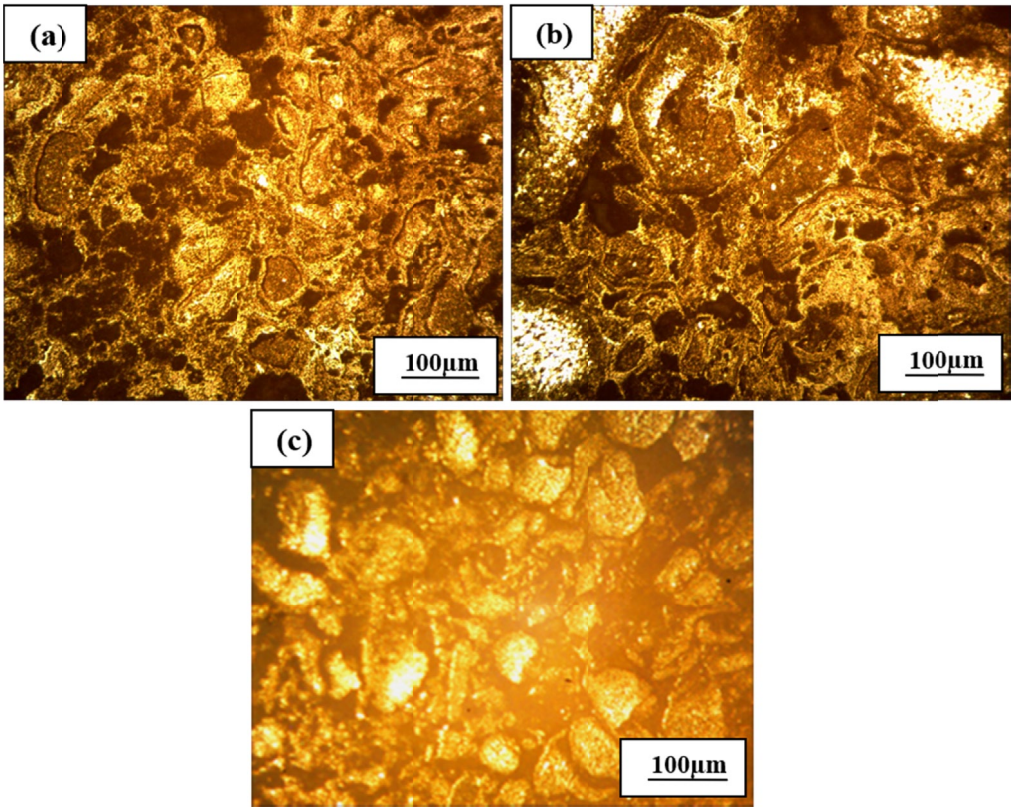

Fig. 4. Optical Micrographs of (a) Ti-35Nb-4Sn alloy, (b) Ti-15Nb-5Zr-4Sn alloy and (c) and Ti-35Nb-7Zr-4Sn alloy

zirconium content also strengthened the material. Li et al. [18] found that adding 12.5Nb-8Zr-2Sn to a composite made of Ti made it stronger and harder. The significant rise in the composites was caused by the increase in the Zr and Sn particles in the filling of pores, which is connected to the reactivity of the Ti-Nb alloy and improving the grain size of the material interface. The material strength and joint efficiency of the composite improved.

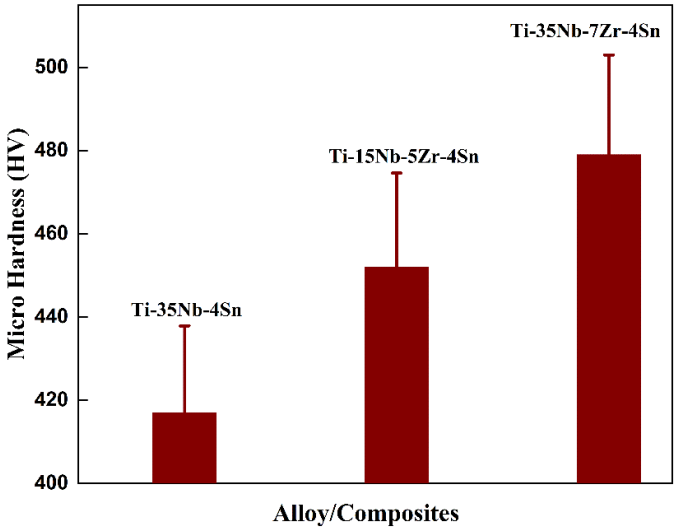

Fig. 5. Graphical representation of microhardness of Ti alloys after sintering and HE

3.2.2. Tensile test

Ultimate tensile strength, percentage of elongation, and yield strength were estimated using a tensile test, and the plots were determined. TABLE 2 represents the tensile strength of Ti-35Nb-4Sn, Ti-15Nb-5Zr-4Sn and Ti-35Nb-7Zr-4Sn alloys. Comparing the Ti-35Nb-4Sn alloy, there is a difference in the increase in ultimate tensile strength of 1042 MPa for Ti-15Nb-5Zr-4Sn composite and 1317 MPa for Ti-35Nb-7Zr-4Sn at the expense of a slight reduction in elongation. The increased tensile strength of this Ti-Nb-Zr-Sn alloy could be attributed to the addition of 35% Nb and 7% Zr particles. However, the Zr and Nb applied to the material surface have drawn more interest recently, which enhanced mechanical properties due to grain refinement. The Ti-Nb combination with Zr and Sn significantly increases the ultimate tensile strength at the expense of a remarkable reduction in elongation. This is due to the presence of Zr and Sn content in the alloy, which leads to reduced agglomeration. Therefore, due to small grains, the highest ultimate tensile strength of 1603 MPa is obtained in the Ti-35Nb-7Zr-4Sn sample. Li et al. [19] studied the mechanical properties of Ti-Nb alloy. The tensile results showed that the ultimate tensile of the Ti-Zr-Nb-Sn bearing alloy was significantly increased, i.e., the increase in tensile strength is 38% higher than the other alloys.

3.2.3. Impact test

The samples for the impact test were prepared as per the ASTM A370 standards using a Charpy impact test machine at room temperature. The three samples were conducted for each alloy, and the average values are reported in the results. The room-temperature impact energy of titanium with niobium samples in the powder condition is reported in Fig. 6. The impact energy of the Ti-35Nb-4Sn alloy is 11 J/m^2, and the impact addition of Zr particles ranges from 15 J/m^2 (Ti-15Nb-5Zr-4Sn) to a maximum of 18 J/m^2 (Ti-35Nb-7Zr-4Sn alloy), respectively. The presence of Zr particles with Ti-Nb leads to improving the impact strength. Yang et al. [20] reviewed the effect of individual Nb elements and a combination of Zr and Sn particles on the toughness of the Ti alloy. It also reported that the impact energy before the coating was observed to be very low in the micro-alloyed samples compared to the coated samples due to the presence of nitride residues, which are severely prone to brittle behaviour under the application of sudden loading.

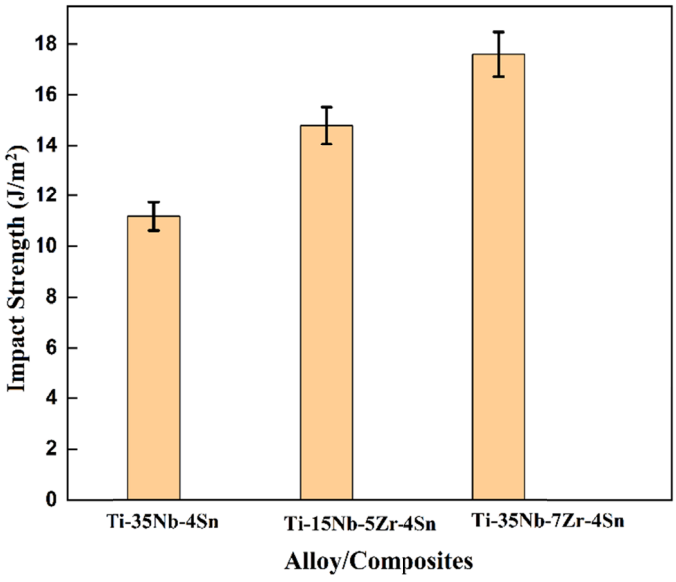

Fig. 6. Impact strength of Ti alloy with Nb content

TABLE 2

Tensile strength of niobium mixtures

Material Composition	Tensile strength (MPa)	Yield Stress (MPa)	Percentage Elongation (%)
Ti-35Nb-4Sn alloy	1042	983	13.26
Ti-15Nb-5Zr-4Sn alloy	1317	1067	9.73
Ti-35Nb-7Zr-4Sn alloy	1603	1291	8.29

3.3. Wear analysis

3.3.1. Effect of applied load on wear loss

The Ti-15Nb-5Zr-4Sn alloy decreases wear loss compared to Ti-35Nb-4Sn alloy due to an interfacial bond between particles which improves wettability. Fig. 7(a) shows that the lowest wear loss is observed at all loads for Ti-35Nb-7Zr-4Sn alloy. This is due to the increased weight fraction of Zr and Nb hard particles. Similar observations were obtained by Hua et al. [21]. The wear loss of Ti-35Nb-4Sn alloy is high (0.102 g) than that of A356/RHA-Fly ash hybrid composites. The addition of 15Nb-5Zr-4Sn with Ti alloy shows a decrease in wear loss of 0.076g (26.3%↓), respectively. Increasing the 35% of Nb and 7% of Zr with Ti alloy exhibited the lowest wear loss of 0.024g (43.2%↓). The Ti-35Nb-7Zr-4Sn alloy, which contains a high concentration of zirconium and niobium content, increases wear resistance by showing reduced wear loss compared to other composites. The representation of Ti-Nb alloy is Ti-35Nb-7Zr-4Sn alloy < Ti-15Nb-5Zr-4Sn alloy < Ti-35Nb-4Sn alloy.

3.3.2. Effect of applied load on the coefficient of friction

The Ti-35Nb-4Sn alloy exhibits abrasive wear at a constant sliding speed of 3 m/s and a sliding distance of 1200 m due to an increased applied load. Increasing the load results in a high frictional force; this force is not equivalent to the increase in load. When the addition of Zr particles increases, COF will increase due to an increase in the area of contact. The friction coefficient is lower by adding 35% Nb and 7% Zr with Ti alloy due to less heat generated at the initial load and varies within the narrow range of 0.21μ (32.7%↓) as shown in Fig. 7(b). At a load of 30N, Ti-35Nb-7Zr-4Sn exhibits a lower friction coefficient (0.26-0.31μ) attributed to increasing hard particles in the matrix compared to the other alloys. The coefficient of friction for Ti-35Nb-4Sn alloy is 0.58 μ and Ti-15Nb-5Zr-4Sn is 0.46 μ, respectively. Increasing the reinforcement of 35% Nb and 7% Zr with Ti alloy exhibited the lowest coefficient of friction. Therefore, the Ti-35Nb-7Zr-4Sn alloy composite is subject to less wear debris and shows better wear resistance and a lower COF.

3.3.3. Specific wear rate of titanium alloys

The specific wear rate of the Ti-35Nb-7Zr-4Sn alloy is three times lower when compared with the Ti-35Nb-4Sn material under all loadings. It happens because the presence of Zr and Sn particles makes it more resistant to wear and tear. The specific wear rate of Ti-35Nb-4Sn alloy is 0.23×10^{-3} mm^3/N-m. It is improved by adding Zr in Ti-15Nb-5Zr-4Sn alloy and increasing Nb particles in Ti-35Nb-7Zr-4Sn alloy from 0.17×10^{-3} mm^3/N-m and 0.12×10^{-3} mm^3/N-m, respectively. As shown in Fig. 8(a), adding Zr, Sn, and Nb to Ti has better wear resistance than other compositions. While Acharya et al. [22] examined the wear rate and COF of niobium alloys, they found that as the volume fraction of Nb and Mo increased, the wear rate and cumulative friction coefficient improved. The variation of wear loss and coefficient of friction of all three alloys is represented in Fig. 8(b-c). It is observed that an increase in Zr and Nb content results in reduced wear loss and COF of the Ti-35Nb-7Zr-4Sn alloy compared to other alloys.

3.4. S-N graphs of notched and Unnotched samples

Fatigue tests are conducted for all alloys at three different stress levels of 80, 100, and 120 MPa with a frequency of 15 Hz and a stress ratio of 0.1. When the stress cycles are limited, a failure S-N curve appears as the specimen is subjected to increasingly large stresses. Fatigue behaviour is highly sensitive to even slight changes in the stress level and fatigue environment

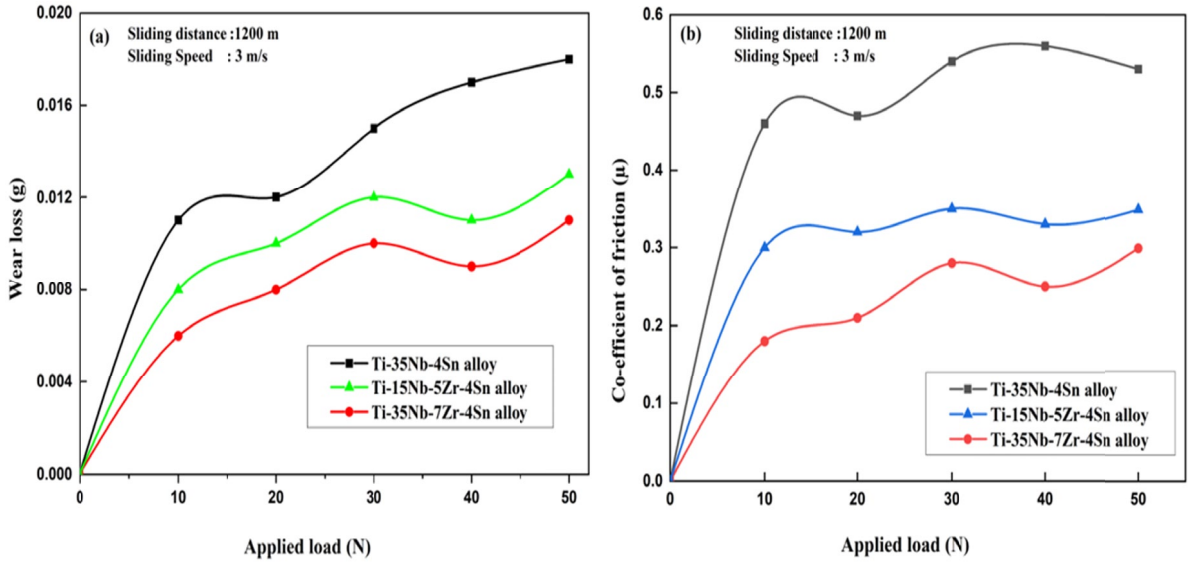

Fig. 7. (a) Wear loss, and (b) Coefficient of friction for various applied load

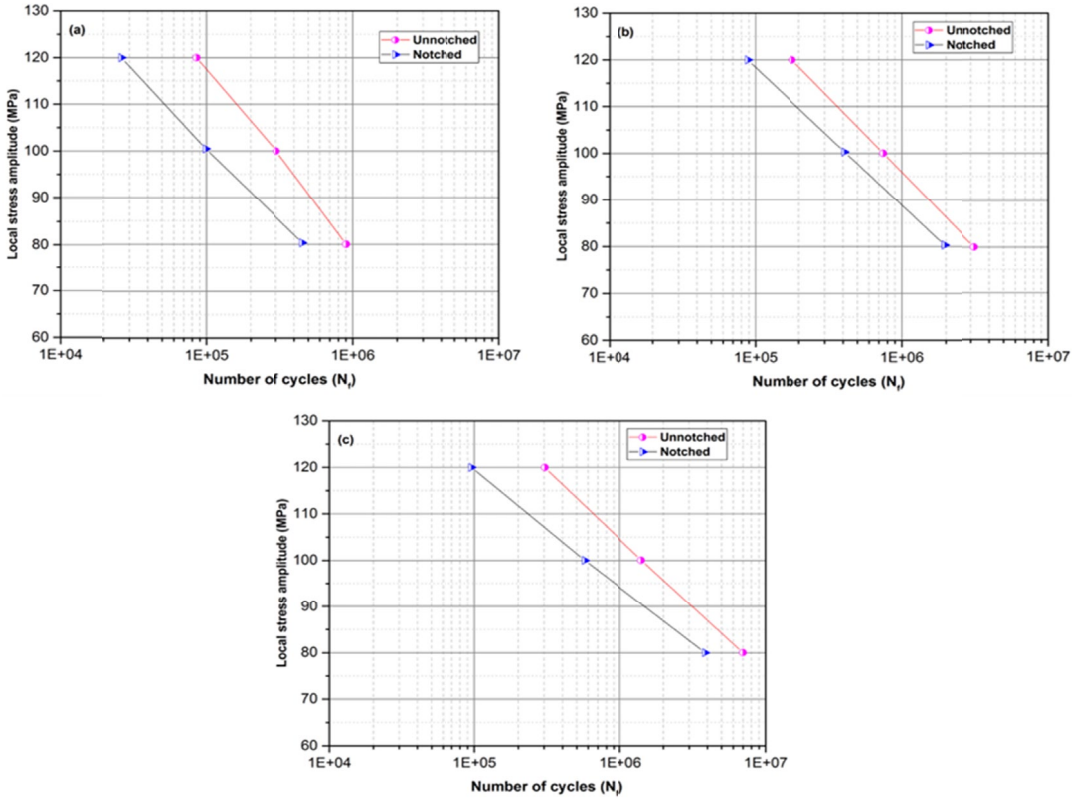

Fig. 8. (a) Specific wear rate, (b) Wear loss vs different weight ratios, and (c) COF vs different weight ratios

that make up a cyclic pattern. Fig. 9(a-c) shows that when the stress amplitude increases, the number of cycles (N) decreases, and new fracture modes arise in various places. The fatigue strength of the three alloys is determined by plotting the S-N curve between the stress range and the number of cycles. When comparing experimental data, the S-N curve is plotted. A relatively small number of cycling attempts generated the initial high stress of 120 MPa. Internal fractures appeared with a stress of

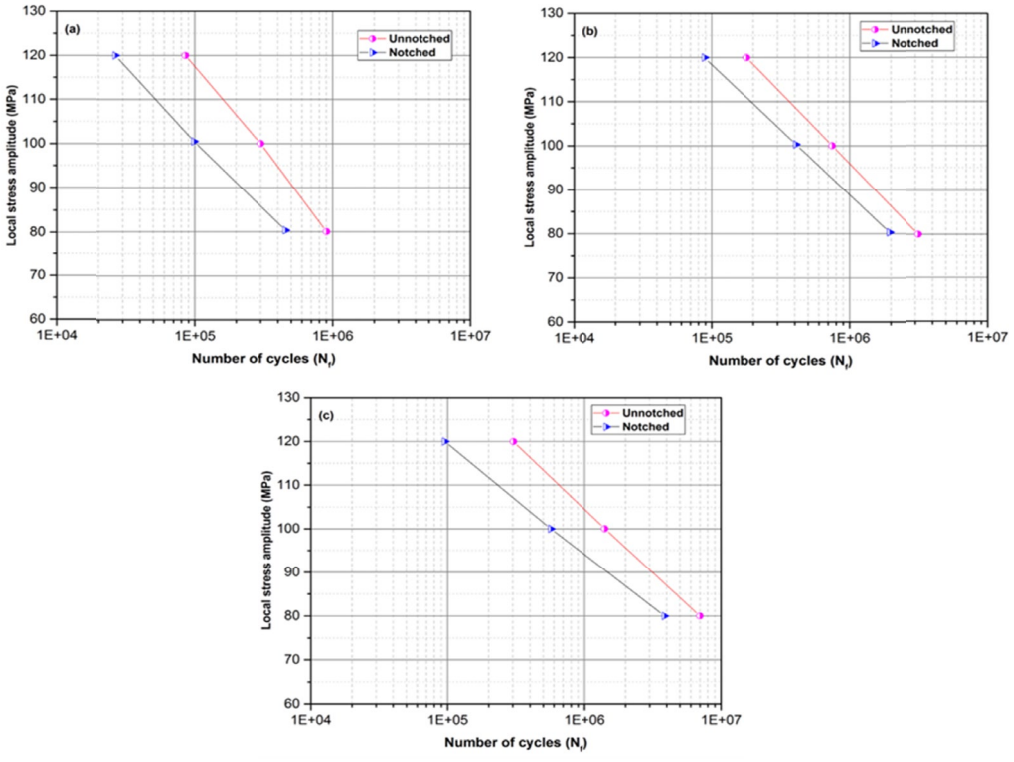

Fig. 9. S-N graphs for notched and Un-notched samples of (a) Ti-35Nb-4Sn alloy, (b) Ti-15Nb-5Zr-4Sn alloy and (c) and Ti-35Nb-7Zr-4Sn alloy

80 MPa, suggesting an abrupt failure mode. At an applied load of 100 MPa, further flaws were visible in the notched specimen but not in the unnotched specimen. The term non-defect failure defines this type of fatigue crack [23]. Thus, the unnotched specimen has more cycles at all stress levels than the notched specimen. When comparing the notched and unnotched specimens, the S-N graph in Fig. 9 reveals that the notched specimen has low cycles (a-c). Ti-35Nb-4Sn alloy has a maximum cycle count of 5.2×10^6 cycles. The maximum cycles for the alloys developed, Ti-15Nb-5Zr-4Sn and Ti-35Nb-7Zr-4Sn, are 7.2×10^6 and 8.5×10^6, respectively. The fatigue life of the Ti-35Nb-7Zr-4Sn composite is increased at all stress levels, which is attributed to its large number of cycles. However, it has been observed that the incorporation of a high percentage of Zr and Nb particles into the Ti has no negative effect on the material and results in an increase in the material's strength compared to other alloys, making it suitable for applications such as turbine blade fabrication and the creation of bio-implants. The Ti-35Nb-7Zr-4Sn alloy outperforms by 30% improvement in strength and endures many cycles than other alloys.

3.5. Surface morphology

SEM (Model: CX-200TM) was used to investigate the topography of Ti-Nb composites, the nature of failure, and the compatibility between the alloys. After fatigue analysis, the cut samples are taken to prepare for SEM examinations, as shown in Figs. 10-12. Further, the unnotched surfaces of the fatigue samples were investigated using the same methodology. At a working distance of 6 mm, the samples were scanned in SEM by an electron beam with an accelerating voltage of

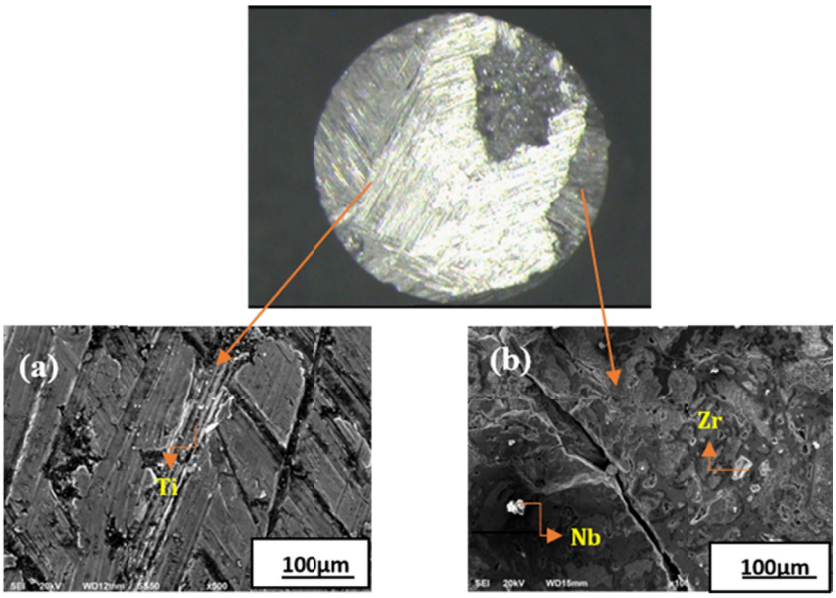

Fig. 10. SEM images of microscopic and macroscopic of the notched specimen of Ti-35Nb-4Sn alloy

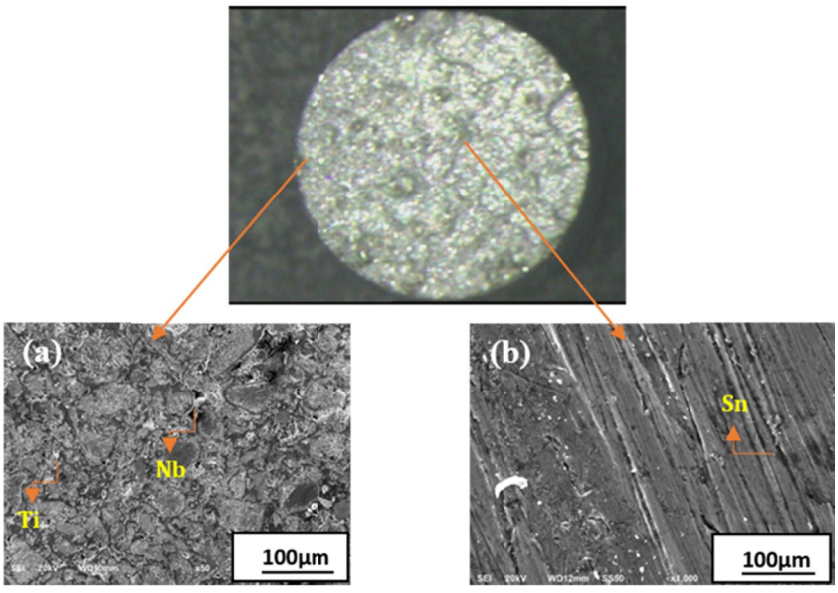

Fig. 11. SEM images of microscopic and macroscopic of the notched specimen of Ti-15Nb-5Zr-4Sn alloy

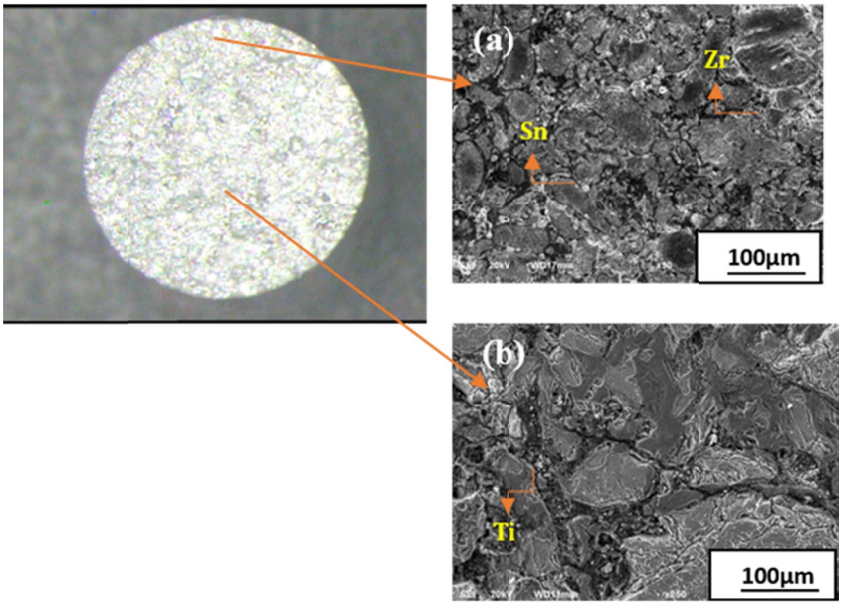

Fig. 12. SEM images of microscopic and macroscopic of the notched specimen of Ti-35Nb-7Zr-4Sn alloy

20 keV and a probe current of 1.0 nA. The cross-sectional image (Ti-35Nb-4Sn) shows the fracture surface is in linear shape due to high agglomeration and poor hardness, as shown in Fig. 10. The outer surface structure of the Zr and Nb particles plays a key role in interfacial bonding between particles, which influences the composites' strength and is shown in Fig. 11(a-b). At the same time, the increase in the weight percent of Nb and Zr particles (Fig. 12) minimises the powder defects (low cracks). The better and more homogenous distribution of Nb and Zr particles in the Ti is attributed to the compact action created by the P/M. Dan et al. [24] revealed that adding Nb-Zr-Sr with Ti as a wetting agent has also proven beneficial for improving wettability, reducing voids, and improving strength, which is necessary for orthopaedic applications. Incorporating nanoparticles into the composite mixture has increased the heat transfer rate and created a more intimate bond between the composite and the mould interface. Adding aligned Ti particles to Zr/Nb/Sn can minimize the cracks and fracture surface. Since the entire proportion of reinforcement particles was added to the vortex formed in the molten matrix, Ti-35Nb-7Zr-4Sn alloy is homogeneously distributed in the matrix, as shown in Fig. 12(a-b). However, a uniform surface with few impurities and non-cellulosic materials is preferred for good interfacial bonding. This could be achieved by adding Zr particles on the surface and the addition of other hard particles.

3.6. XRD analysis

An X-ray diffractometer was used to capture the X-ray diffractograms as per ASTM 3419-22 standards for all three composites, as shown in Fig. 13(a-c). A higher crystalline index obtained for Ti-35Nb-4Sn alloy could be attributed to the structure's

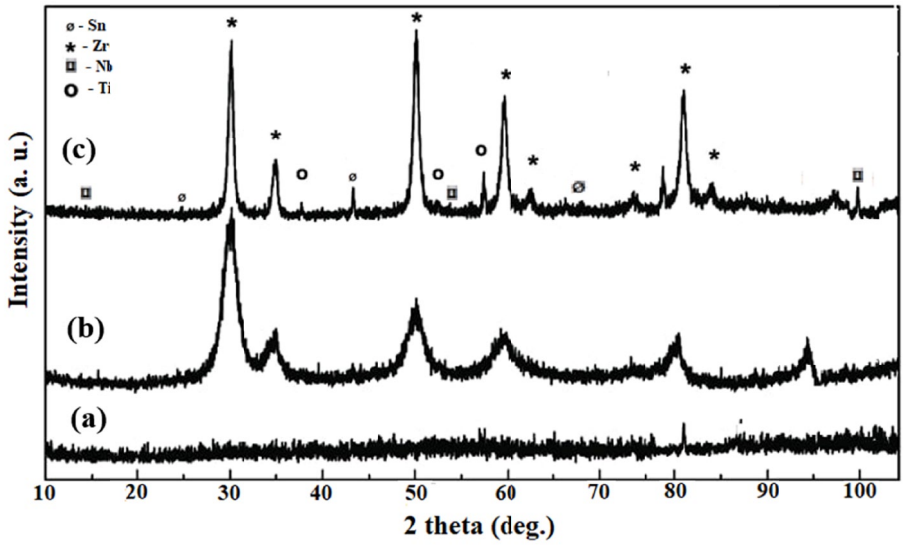

Fig. 13. XRD analysis of (a) Ti-35Nb-4Sn alloy, (b) Ti-15Nb-5Zr-4Sn alloy and (c) and Ti-35Nb-7Zr-4Sn alloy

regular atom arrangement. The sharp peaks at 2Θ = 42.9°, 62°, and 73.8° indicated the crystal structure as shown in Fig. 13(a). When 5Zr particles are added to the Ti-Nb-Sn alloy, the lowering peak confirms the addition of carbon, zirconium, and iron content. In all the substances, a significant peak in absorption from the spectra was initially observed between ranges of 55.6° and 92.3°, indicating the crystalline form of the substances. Cordeiro et al. [25] concluded that increasing Zr and Nb particles to the Ti alloy could cause an essential phase to form at the alloy-particle interface during annealing, making the material more resistant to corrosion and wear. The XRD curve for Ti-35Nb-7Zr-4Sn alloy (Fig. 13(c)) was two prominent peaks at 43.07° and 80.16°, indicating that the reinforcement particles are semi-crystalline.

4. Conclusion

The Ti-Nb-Zr-Sn alloys are used in orthopaedic, aerospace, and structural applications, apart from their extensive applications in defence. In this study, Ti-Nb alloys were successfully fabricated through the powder metallurgy process. From the above tests and analyses, the following conclusions are drawn:

1. The OM images demonstrated the presence of refined grains, fragmented phases, and homogeneously dispersed Zr particles in the composite. The average grain size and smooth surface fracture are obtained in the Ti-35Nb-7Zr-4Sn alloy, which is better than the other alloys.
2. The hardness is improved from 438.71 HV to 479.83 HV (Ti-35Nb-7Zr-4Sn) due to the presence of Zr and Nb particles that strongly attract Ti leads, improving the strength.
3. Tensile test results established with the Ti in combination with 35% Nb/7% Zn increase the ultimate tensile strength significantly at the expense of a remarkable reduction in elongation up to 17%. The Ti-35Nb-4Sn has the lowest ultimate tensile strength of 1042 MPa among the samples. It is due to the Sn content in the soft ferrite matrix, which leads to agglomeration. The highest ultimate tensile strength of 1603 MPa is obtained in the Ti-35Nb-7Zr-4Sn sample due to very fine bcc grains compared to other alloys. The test results and characterization all point to the Ti-35Nb-7Zr-4Sn composite being a good material for bioimplant applications.
4. The impact energy of the Ti-35Nb-4Sn alloy is 11 joules, and the impact after adding Zr particles ranges from 11 joules to a maximum of 15 joules. While applying the 7% of Zr and 35% of Nb exhibits highest impact energy of 18 joules.
5. Due to the addition of Ti-35Nb-7Zr-4Sn shows more consistent flow stability regimes than the other alloy for all test conditions. Comparing S-N graphs of notched and unnotched specimens, the peaks and plateaus caused by strain hardening and flow softening occur at different stress levels.
6. Compared to Ti-35Nb-4Sn alloy, the wear loss of Ti-15Nb-5Zr-4Sn with various applied load are less. The Ti-15Nb-5Zr-4Sn alloy shows a decrease in wear loss (26.3%↓). Increasing the Nb and Zr particles (Ti-35Nb-7Zr-4Sn alloy) exhibited the lowest wear loss (78.2%↓). Similar observations are found in COF is decreased to 25.3% compared to other alloys.
7. The microscopic examination shows that the Zr, Sn and Nb alloying elements are distributed homogenously within Ti alloy. Therefore, it is concluded that Ti-35Nb-7Zr-4Sn alloy is the best-suited material for biodegradable implant applications.

REFERENCES

[1] J. Li, X. Cui, G.J. Hooper, K.S. Lim, T.B. Woodfield, Rational design, bio-functionalization and biological performance of hybrid additive manufactured titanium implants for orthopaedic applications: A review. J. Mech. Behavior Of Biomed. Mater. **105**, 103671 (2020).

[2] K. Ronoh, F. Mwema, S. Dabees, D. Sobola, Advances in sustainable grinding of different types of the titanium biomaterials for medical applications: A review. Biomed. Eng. Adv. **22**, 100047 (2022).

[3] Z.H. Wen, W.A. Yao, W.M. Chen, L.J. Zhang, D.U. Yong, Investigation of mechanical and diffusion properties in bcc Ti-Nb-Zr-Sn alloys via a high-throughput method. Trans. Nonferrous Met. Soc. China **31** (11), 3405-15 (2021).

[4] Y. Lee, S. Li, E.S. Kim, D.J. J.B. Lee, Seol H. Sung, H.S. Kim, T. Lee, J.S. Oh, T.H. Nam, J.G. Kim, Transformation-induced plasticity in the heterogeneous microstructured Ti-Zr-Nb-Sn alloy via in-situ alloying with directed energy deposition. Additive Manuf. **58**, 102990 (2022).

[5] Y. Alshammari, Y. Alkindi, B. Manogar, F. Yang, L. Bolzoni, Zr-bearing powder metallurgy binary Ti alloys: Fabrication and characterisation. Mater. Sci. & Eng. A. **853**, 143768 (2022).

[6] S. Suresh, B. Vinod, K.S. Sujith, D. Sudhakara, Investigation and performance of high niobium contain Ti-Al Alloys: Deformation behaviour and microstructural evolution. Mater. Today: Proceed. **63**, 427-432 (2022).

[7] A. Balikai, H. Adarsha, R. Keshavamurthy, Microstructure and Nanoindentation response of Si3N4-Reinforced Magnesium-based Composite Synthesized by Powder Metallurgy Route. J. Inst. Eng. (India): Series D. **103** (1), 235-47 (2022).

[8] P. Mondal, A. Das, A. Mondal, A.R. Chowdhury, A. Karmakar. Fabrication of Ti-6Al-4V Porous Scaffolds Using Selective Laser Melting (SLM) and Mechanical Compression Test for Biomedical Applications. J. Inst. Eng. (India): Series D. **103**, 181-190 (2022).

[9] Y. Chen, X. Sun, T. Zhang, C. Han, X. Ye, X. Liu, Y. Zhao, L. Zhang, G. Zeng, A. Aizaz. Tribological performance study of zirconium phosphate as an additive in titanium complex grease. Mater. Letters. **321**, 132402 (2022).

[10] B. Vinod, M. Anandajothi, Dry sliding wear mechanisms of incorporated hydroxyapatite waste materials: synthesis and characterization of magnesium hybrid composites. Trans. Indian Inst. Metals. **73** (12), 3037-57 (2020).

[11] E. Aygul, S. Yalcinkaya, Y. Sahin, Characterization of Ti-6Al-(4V-7Nb-4Mo) Biomedical Alloys Produced by Powder Metallurgy Method. Powder Met. & Met. Ceramics. **59** (5), 296-302 (2020).

[12] B. Vinod, S. Suresh, S. Reddy, K.S. Sujith, Tribological and Mechanical Characteristics of Mg-Zn6. 0-Y1. 2-Zr0. 2 alloy by SPS Technique: Natural and Agro-Waste Utilization. J. Bio-and Tribo-Corr. **9**(1), 1-6 (2023).

[13] S.M. Nur, M.H. Parveg, S. Ahmed, N.R. Dhar, Experimentation on Enhancing Mechanical Characteristics of E-glass Fiber-Strengthened Epoxy Resins with Fillers. J. Inst. Eng. (India): Series D. **103**, 513-522 (2022).

[14] S. Li, H. Yu, Y. Lu, J. Lu, W. Wang, S. Yang, Effects of titanium content on the impact wear properties of high-strength low-alloy steels. Wear **474**, 203647 (2021).

[15] S. Suresh, D. Sudhakara, B. Vinod, Investigation on mechanical, wear, and machining characteristics of Al 7075/MWCNTs using the liquid state method. Adv. Comp. & Hybrid Mater. **3** (2), 243-54 (2020).

[16] S. Ramanathan, B. Vinod, M. Anandajothi, Effect of organic and inorganic reinforced particulates for fatigue behaviour of Al-Si7-Mg0. 3 hybrid composite: V-notched and un-notched specimen experiments with microstructural constituents. SN App. Sci. **1** (1), 1-6 (2019).

[17] S. Li, J.H. Lim, I.U. Rehman, W.T. Lee, J.G. Kim, J.S. Oh, T. Lee, T.H. Nam, Tuning the texture characteristics and superelastic behaviors of Ti-Zr-Nb-Sn shape memory alloys by varying Nb content. Mater. Sci. & Eng: A. **845**, 143243 (2022).

[18] S. Li, Y.W. Kim, M.S. Choi, J.G. Kim, T.H. Nam, Superelasticity, microstructure and texture characteristics of the rapidly solidified Ti-Zr-Nb-Sn shape memory alloy fibers for biomedical applications. Mater. Sci. & Eng: A. **831**, 142001 (2022).

[19] Z. Li, M. Chen, W. Li, H. Zheng, C. You, D. Liu, F. Jin, The synergistic effect of trace Sr and Zr on the microstructure and properties of a biodegradable Mg-Zn-Zr-Sr alloy. J. Alloys & Comp. **702**, 290-302 (2017).

[20] Y. Yang, X. Guo, Z. Dong, Effect of Nb on microstructure and mechanical properties of Ti-xNb-4Zr-8Sn alloys. Mater. Sci. & Eng. A. **825**, 141741 (2021).

[21] N. Hua, W. Wang, Q. Wang, Y. Ye, S. Lin, L. Zhang, Q. Guo, J. Brechtl, P.K. Liaw, Mechanical, corrosion, and wear properties of biomedical Ti-Zr-Nb-Ta-Mo high entropy alloys. J. Alloys & Comp. **861**, 157997 (2021).

[22] S. Acharya, A.G. Panicker, D.V. Laxmi, S. Suwas, K. Chatterjee, Study of the influence of Zr on the mechanical properties and functional response of Ti-Nb-Ta-Zr-O alloy for orthopedic applications. Mater. & Design. **164**, 107555 (2019).

[23] A.A. Shanyavskiy, A.P. Soldatenkov, Crack growth regularities and stress equivalent for in-service fatigued fan disk of titanium alloy Ti-6Al-3Mo-2Cr. Inter. J. Fatigue. **162**, 106956 (2022).

[24] A. Dan, E.M. Cojocaru, D. Raducanu, I. Cinca, V.D. Cojocaru, B.M. Galbinasu, Microstructure and mechanical properties evolution during thermomechanical processing of a Ti-Nb-Zr-Ta-Sn-Fe alloy. J. Mater. Res. & Tech. **19**, 2877-87 (2022).

[25] J.M. Cordeiro, B.E. Nagay, A.L. Ribeiro, N.C. da Cruz, E.C. Rangel, L.M. Fais, L.G. Vaz, V.A. Barão, Functionalization of an experimental Ti-Nb-Zr-Ta alloy with a biomimetic coating produced by plasma electrolytic oxidation. J. Alloys & Comp. **770**, 1038-48 (2019).